

A0804 (Candidate EFCF Special Issue, www.EFCF.com/LIB)

Benchmark Study of Performances and Durability between Different Stack Technologies for High Temperature Electrolysis

**Jerome Aicart (1), Alexander Surrey (2), Lucas Champelovier (1), Kilian Henault
(1), Chistian Geipel (2), Oliver Posdziech (2), Julie Mougín (1)**

(1) Univ. Grenoble Alpes, CEA, Liten, DTCH, 38000 Grenoble/France

(2) Sunfire GmbH, 2 Gasanstaltstraße, D-01237 Dresden/Germany

Tel.: +33-43878-6744

jerome.aicart@cea.fr

Abstract

In the current landscape of High Temperature Electrolysis (HTE), two Solid Oxide Cell (SOC) technologies are being used: electrolyte-supported and cathode-supported SOCs. The geometrical differences, namely the thickness of the electrolyte, can lead to vastly different operating temperatures. Since most phenomena affecting performance and durability remain thermally activated, comparing stack technologies can be a difficult endeavor at best.

While the most visible goal of the European project MULTIPLHY consists of Sunfire GmbH building the first multi-megawatt (~2.4 MW) Solid Oxide Electrolyzer (SOEL), a work package is being dedicated to stack testing in a laboratory environment. A harmonized testing protocol was elaborated specifically to allow comparing different stack technologies. It includes the recording of performance maps, several durability steps in thermoneutral galvanostatic operation, as well as load point and thermal cycles, resulting in a minimum test duration of 4,000 hours. Subsequently, Sunfire operated two 30-cell electrolyte-supported stacks for over 8,200 hours, while a 25-cell cathode-supported stack was tested at CEA for 6,800 hours.

The present report aims at presenting the findings gathered during the implementation of the harmonized protocol. This benchmark study puts forward performance maps as well as voltage and stack temperature profiles over time, and discusses some of the difficulties inherent to long-term testing.

Introduction

The shift to a low-carbon EU economy raises the challenges of integrating renewable energy sources (RES) and cutting the CO₂ emissions of energy intensive industries (EII). In this context, hydrogen produced from RES will contribute to decarbonize those industries, as feedstock/fuel/energy storage. MULTIPLHY thus aims to install, integrate and operate the world's first high-temperature electrolyser (HTE) system at a multi-megawatt-scale (~2.4 MW). Located in Rotterdam, its hydrogen production ($\geq 60 \text{ kg}\cdot\text{h}^{-1}$) will feed the chemical processes of a renewable products refinery.

With its rated electrical connection of ~3.5 MW_{el,AC,BOL}, electrical rated nominal power of ~2.6 MW_{el,AC} and a hydrogen production rate $\geq 670 \text{ Nm}^3\cdot\text{h}^{-1}$, this HTE will cover ~1 % of the current average hydrogen demand of the refinery. MULTIPLHY's electrical efficiency (85 %_{el,LHV}) will be at least 20 % higher than efficiencies of low temperature electrolyzers, enabling the cutting of operational costs and the reduction of the connected load at the refinery and hence the impact on the local power grid.

A multidisciplinary consortium gathers NESTE (a renewable products refiner as end-user), ENGIE (a global energy system integrator & operator), Paul Wurth (Engineering Procurement Construction Company for hydrogen processing units), Sunfire (HTE technology provider) and the Research and Technology Organisation (RTO) CEA. They focus on operation under realistic conditions and market frameworks to enable the commercialisation of the HTE technology. By demonstrating reliable system operation with a proven availability of $\geq 98 \%$, complemented by a benchmark study for stacks in the 2-to-5 kW range, critical questions regarding durability, robustness, degradation as well as service and maintenance will be addressed.

1. Scientific Approach

The present work focuses on benchmarking two stack technologies: one from CEA incorporating cathode-supported cells (CSC), and one with electrolyte-supported cells (ESC) by Sunfire. CSCs rely on thick porous H₂ electrodes to provide the cells with mechanical support, while ESC are comprised of comparatively thicker electrolytes. The choice of cell architecture and materials defines nominal current densities, and dictates the operating temperature at the beginning-of-life of the stack: CSCs are typically operated around 700-750°C, and ESCs around 800-850°C. Despite these differences, special attention was initially devoted to formulate a harmonized protocol which allowed for comparing the performances and the degradation rates of the stack technologies.

Throughout all galvanostatic operation segments, the steam conversion was kept constant at 70%, a value relevant for the industrialization of the technology. In addition, stack voltage was maintained close to the thermoneutral value (approximately 1.29 V per cell at 750°C), to reduce thermal gradients in the stack. As a result, the only remaining parameter, the stack temperature, was adjusted so that the previous targets were met. Under constant load, as the stack degrades over time, the voltage increases. Consequently, the stacks temperature was regularly increased to compensate for the degradation and maintain the cells in (near) thermoneutral operation.

The complete protocol is publicly available on MULTIPLHY website [1]. It includes the recording of initial and final performance maps, durability steps in galvanostatic and quasi-potentiostatic operation, load point and thermal cycles.

2. Experiments

2.1.CEA Stack Description

Commercial $12 \times 12 \text{ cm}^2$ electrode-supported cells with an active area of 100 cm^2 were used in this work. All cells were identical, exhibiting a Ni-8YSZ cermet fuel electrode, an 8YSZ electrolyte, a CGO diffusion barrier and a LSC oxygen electrode.

The 25-cell stack incorporated thin AISI441 ferritic stainless steel interconnects with proprietary design, allowing cross-flow operation. Optimization of gas distribution has led to significant increase of achievable conversion rates [2]. Tightness between compartments was achieved with a combination of ceramic glass seals, mica foils, and an integrated stand-alone clamping system [3] for mechanical load. Finally, electrical contacts between electrodes and interconnects were insured through nickel grids on the hydrogen side, and LSM on the oxygen side. The stack gas connections to the test bench were done through an in-house developed solution based on a form of high temperature flanges. Additional information on stack design and experimental results on performance and durability can be found in references [4–10].

2.2.CEA Testing Equipment and Deviations from the Protocol

Stack assembly from in-house manufactured components, as well as glass formation and cermet reduction procedures were carried out on a dedicated stack conditioning bench co-developed between company ECM and CEA. Subsequently, it was transferred to a reversible lab system (Figure 1) incorporating Balance of Plant (BoP) components, such as heat exchangers for heat recuperation, for the actual test sequence. Details about the testing equipment can be found elsewhere [8], [11], [12].

The drop-down furnace incorporates one lateral heating element and another on top, and is positioned above the rest of the bench BoP. To overcome the known vertical (top-to-bottom) temperature gradient in the furnace, which could jeopardize isothermal operation, the stack was manufactured with an Integrated Stack Heating Solution (ISHS), described in Reference [8]. Unfortunately, the bottom part of the ISHS gave out at around 300°C during the first temperature ramp up sequence. The subsequent inability to measure the resistance of the heating element suggests that the manufacturing process may have introduced an air bubble in between the heating element and the electrical insulation material surrounding it. This would have led to extreme local temperatures due to the inability to efficiently extract heat by conduction, and led to the destruction of the heating element and the opening up of the electrical circuit. To overcome this, a high temperature heating wire (maximum temperature 900°C) was wrapped around the inlet gas preheating loops as well as the stack bottom self-clamping element. The overall thermal regulation of the furnace was modified so that only the lateral furnace element was used for temperature control, while the power delivered by the wrapped heating wire was adjusted to nullify the temperature difference between the top and bottom parts of the stack. While quite rudimentary, the implemented final solution led to acceptable results in terms of performance and temperature control. It has remained functional throughout the whole testing sequence.

While performance assessment at 800°C was initially targeted, 765°C was the maximum temperature reachable due to the degraded thermal management. The current ramp rate was increased from 0.05 (SOCTESQA recommendation [13]) to $1 (\text{A.cm}^{-2}).\text{min}^{-1}$. This fast control strategy, successfully implemented in a previous work [14], [15], allowed avoiding significant temperature gradients in the stack when ramping up the stack voltage between OCV and thermoneutral voltage. Finally, no redox cycle was done on the stack, since it was believed it could cause damage that would have hindered post-mortem analyses.

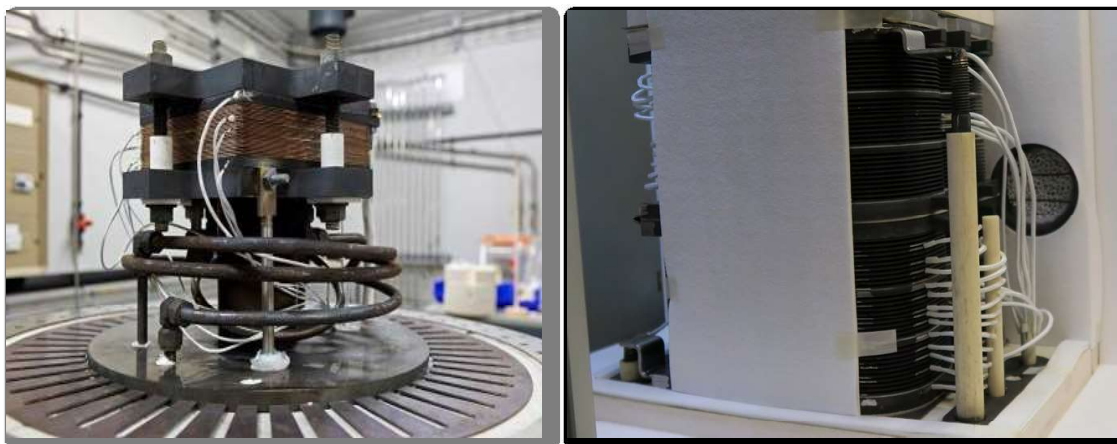


Figure 1: Stack used at CEA (left, [11]), and two-stack pile up installation at Sunfire (right).

2.3. Sunfire Stack Description

The Sunfire SOC stack consists of 30 layers as described in previous publications [16]–[18]. Typically, two of these stacks are piled up and tested together (Figure 1) at the Sunfire test field. The employed electrolyte supported cells (ESC) consist of an 80 μm thick 3YSZ electrolyte, a Ni-GDC hydrogen electrode, a LSCF-GDC oxygen electrode, and have an active area of 127.8 cm^2 . The interconnector is a steel cassette out of Crofer 22 APU with a MCF coating at the oxygen side. The steam/hydrogen mixture is distributed to each layer via internal manifolds, whereas the air side has an open manifold, allowing for a co-flow operation.

2.4. Sunfire Testing Equipment and Deviations from the Protocol

For the reported test, a Fuelcon test bench was used, where a so-called Stack-Test-Box (STB) designed by Sunfire is mounted. In this STB the two stacks are integrated by applying the necessary clamping force, thermally insulating the stacks, and guiding the gases and air through the stacks. No active heating elements are used in the STB, but the stacks are heated by hot air and gases up to 840°C.

Additionally to the defined test protocol, the galvanostatic operation was performed at 70% and 80% steam conversion. The stationary operation has only been done at $-0.5 \text{ A}\cdot\text{cm}^{-2}$, not at $-0.65 \text{ A}\cdot\text{cm}^{-2}$ due to higher than expected ASR (maybe caused by higher initial degradation due to high initial silica contamination or cells batches with higher ASR).

3. Results

3.1. Overview & Time Evolutions

Figure 2 shows the evolution of stack current, voltage, and temperature for both technologies over the complete test sequences. The CSS temperature is defined here as the outlet air temperature, while for the ESS, with their open air compartments, the data relates to the maximum temperature recorded among several sensors inserted inside the stack. A 1,200 h gap is visible on the CSS test, mostly linked to the building annual technical shutdown. It is important to note that aside from the load point cycles, each segment of the protocol is characterized by a steady current (H_2 production) and a steady stack voltage (energy cost at stack level).

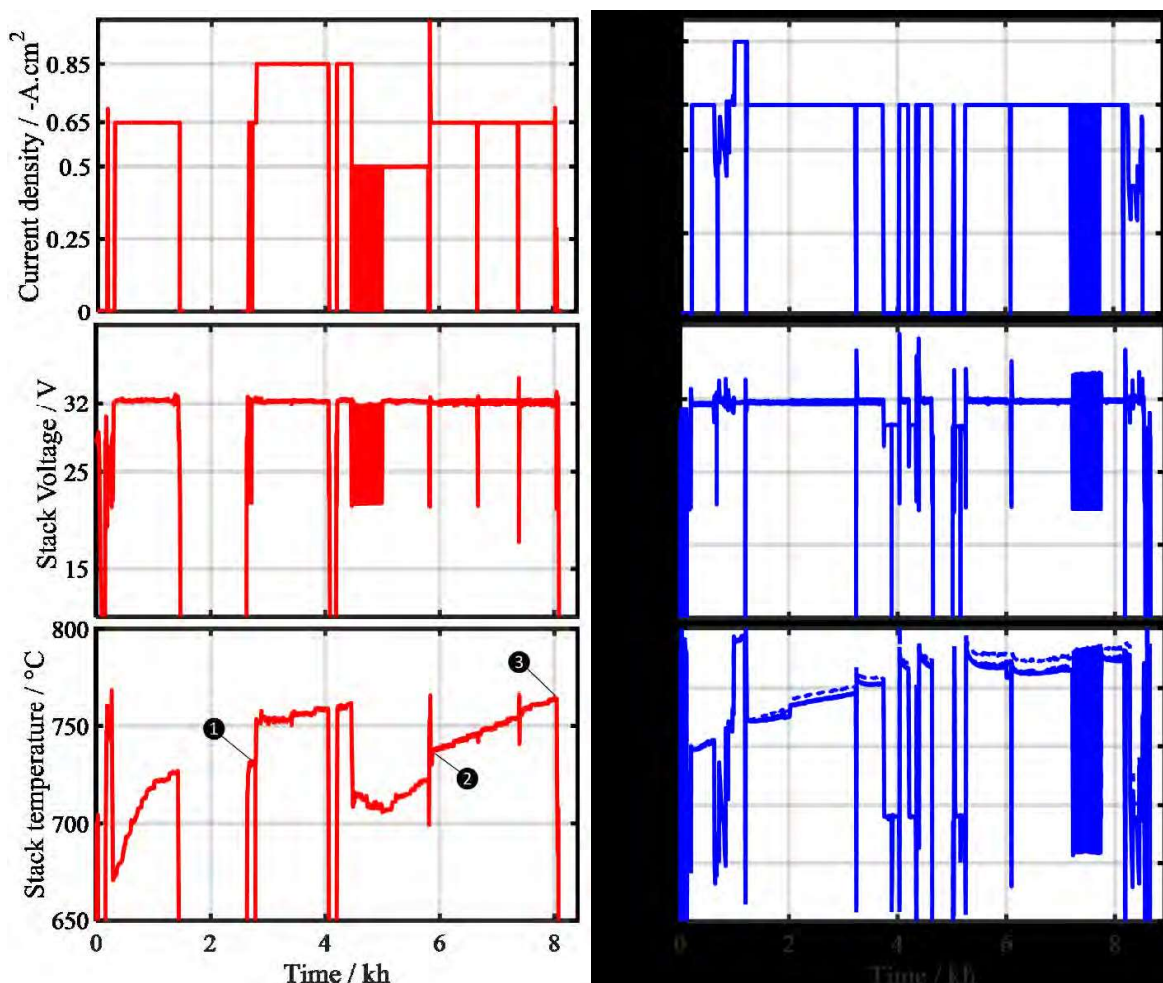


Figure 2: Time evolutions for stack current and voltage for the cathode-supported stack (red, left) and the two electrolyte-supported stacks (blue, right). The maximum temperature of both ESS piled-up is shown (solid and dotted curves).

The ESS went through several unwanted events between 3 and 5 kh, caused by failures of the steam supply, and leading to thermal cycles. These events are discussed in section 3.3.

The CSS underwent two thermal cycles (1.5 & 4 kh), with stack operating conditions being the same before and after to assess potential impacts. These chronologically led to a +3°C and a +1.5°C temperature increases. Beyond the numerical results (surely affected by experimental imprecisions) the impact of the cycles on the performance remained limited. To provide some preliminary estimation about the CSS lifespan, linear regressions were performed between points ① and ② (Figure 1 – 3,100 h segment), as well as between points ② and ③ (2,100 h segment), all points corresponding to operation at -0.65 A.cm⁻². The rates of temperature increase hence calculated were +2.3°C.kh⁻¹ and +12.4°C.kh⁻¹, respectively. Assuming a maximum End-of-Life temperature (T_{EOL}) of 860°C due to the glass seals, these results translated into 60 and 15 kh total stack lifespans at iso-performances, respectively. While the main driver for degradation may have changed between the two segments to explain the vastly different rates, these results highlight at the very least the necessity of actual long-term testing to evaluate stack replacement frequency and properly estimate a consolidated “Levelized Cost Of Hydrogen” (LCOH) [7].

3.2. Performance Maps

From a stable temperature to be investigated, the stacks were polarized from OCV to the thermoneutral voltage to record its performances. From there, if needed, current and flowrates were adjusted incrementally until stack operation resulted in the following observations:

- Average cell voltage ≈ 1.3 V (depending on the temperature)
- Steam conversion = 70%
- Temperature under load ≈ Temperature at OCV

The current density hence identified was recorded, and is denoted “thermoneutral current density at 70% SC”, or THN70, in the following for simplicity.

Figure 2 gathers the i_{THN70} results recorded at CEA and Sunfire at the start and the end of testing sequences. They show that in comparable conditions of temperature, the CSS experienced a significant decrease of the thermoneutral current densities. For example, comparing initial and final performances at about 703°C, the current density allowing near iso-thermal stack operation and 70% steam conversion decreased from -0.83 to -0.30 A.cm⁻², a 63% drop. The extent of the recorded performance drop decreased at higher temperature, going from -1.55 down to -0.65 A.cm⁻² at approximately 765°C (-58%). Evidently, while the recorded degradation remains affected by the temperature of the measurement, the intrinsic stack degradation was identical. Such influence of the temperature on the extent of the recorded performance decrease is also noticeable on the ESS, albeit to a lesser extent. Indeed, thermoneutral current densities went from -0.34 down to -0.23 A.cm⁻² at 780°C (-32%), and from -0.59 to -0.45 A.cm⁻² at 840°C (-24%).

The recorded decrease of CSS performance over time at iso-temperature is quite significant, especially considering the stack was “only” in operation for a few thousand hours. Such impact on the performances would be consistent with degradation rates of several percent per thousand hours typically reported on electrode-supported cells operated in electrolysis and galvanostatic modes [19]. However, the previously reported results of temperature increase over time indicate that the stack could, in theory, be operated for quite some time before reaching its EoL temperature (around 860°C). This shows that with control strategies based on temperature increase to compensate for

degradation, the typical notion of degradation rates measured during potentiostatic or galvanostatic operation at iso-temperature might be misleading when trying to evaluate the lifespan of a cell/stack.

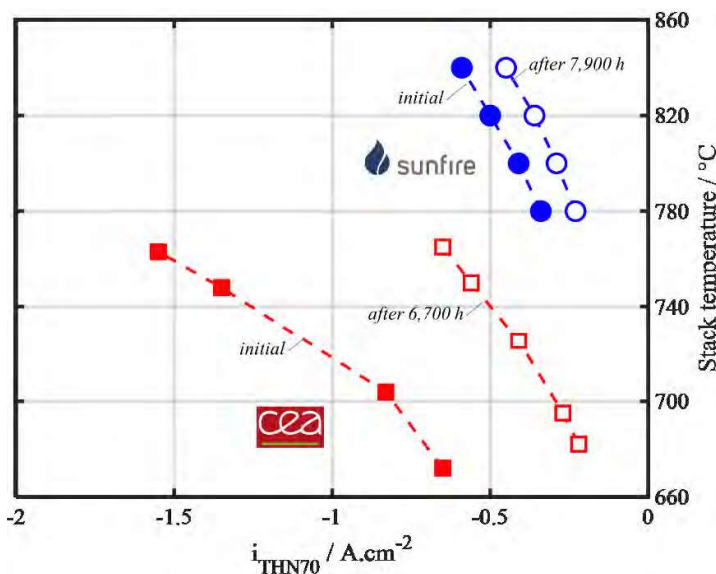


Figure 3: Initial and final performance maps recorded on both stack technologies. THN70 relates to operation at the thermoneutral voltage and at 70% steam conversion.

3.3.Stack Resilience

At approximately 3,400 h, CEA's high temperature laboratory experienced a cut off of the H₂ supply, consequence of a problem with the air extraction. The polarized stack was consequently fed with 100% steam. The gas supply was abruptly restored after 3h30, while the H₂ mass flow controller's valve was fully open. This led to a +300 mbar overpressure event at the bench inlet, as seen in Figure 4. The exact position of the pressure sensors that recorded the event can be found in [12]. Table 1 gathers Open Circuit Voltages (OCV) values measured throughout the test protocol via the eight voltage measurements available on the test bench. As can be seen, no significant impact of the loss of H₂, pure steam operation, and subsequent water head event can be noticed on the stack voltage and OCVs.

Between about 3,000 and 5,000 h, the ESS experienced several unplanned malfunctions of the steam supply, leading to temporary starvation and unwanted thermal cycles (Figure 2). If the short-term performance was impacted, with a noticeably higher thermoneutral temperature at the targeted current density, the stack proved to be resilient, and its response improved rapidly. No significant residual performance drop was consequently recorded. In addition, as part of the protocol, the ESS underwent several Electrochemical Tightness Tests (ETT), during which all gas supplies to the stack are cut-off and the subsequent evolution of cell voltages over time is recorded. This test is rather drastic, and much more efficient in detecting tightness defects than a collection rate assessed through flowrate measurements. The ETT ends either when a voltage measurements passes below a threshold of approx. 0.7 V (nickel oxidation potential), or after 20 minutes, whichever comes first. Figure 4 shows the initial ETT results, and the final ones recorded after a redox cycle. The test results highlight excellent tightness, and the stack's ability to withstand such cycle of Ni oxidation without severely compromising the cell's integrity and performances. The increased voltage drops in 3 blocks indicate small leaks, which were

originally caused by the mentioned malfunctions between about 3,000 and 5,000 h. These events outside of the specified operation points must be avoided to ensure an ideal long-term operation of the stack. Nonetheless, the present leaks did not endanger the further operation and the successful completion of the test.

This paragraph only details some of the failures and malfunctions that occurred during both testing sequences. While not meant to be exhaustive, these examples nevertheless underline the difficulties inherent to long term testing, in spite of CEA and Sunfire extensive testing experience.

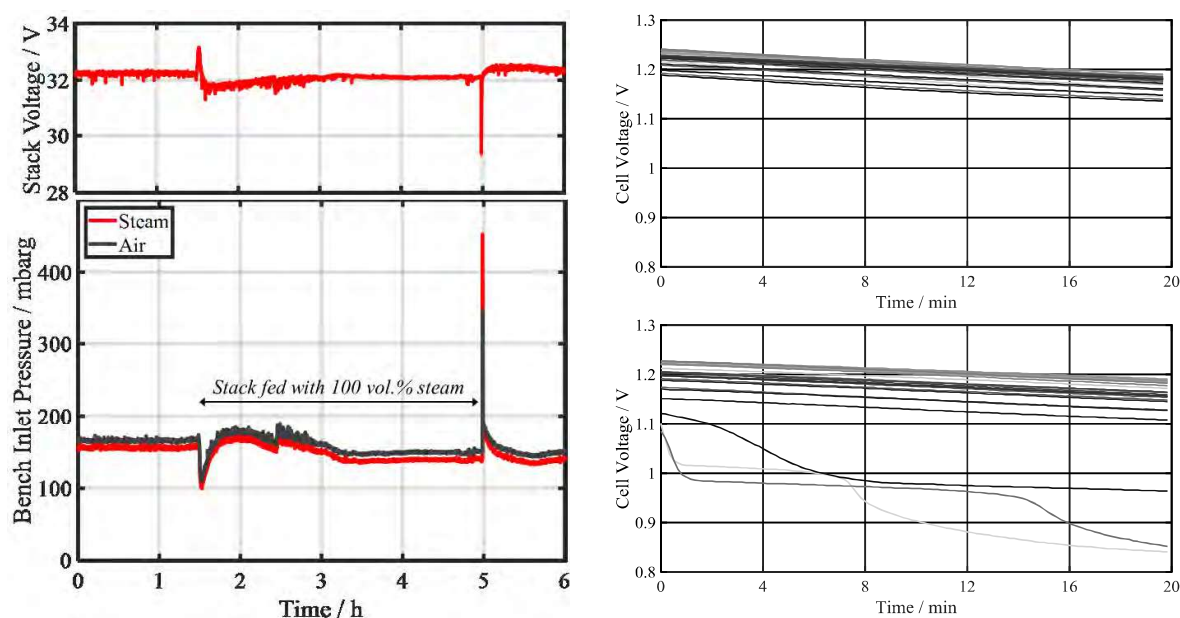


Figure 4: Resilience of both technologies with (left) the CSS response to a temporary cut-off and subsequent abrupt restoration of the H₂ supply leading to an overpressure, and (right) electrochemical tightness test results recorded initially (top) and after a redox cycle (bottom) on the ESS.

Time h	U ₁ mV	U ₂₋₄ mV	U ₅₋₈ mV	U ₉₋₁₂ mV	U ₁₃₋₁₆ mV	U ₁₇₋₂₀ mV	U ₂₁₋₂₄ mV	U ₂₅ mV	T _{AO} °C	OCV _{TH} mV	Δ _{TOT} %
292	888	887	888	888	887	887	888	888	673	892	-0.51%
2,642	870	868	869	869	868	868	868	867	717	873	-0.51%
4,728	870	871	871	871	870	871	872	872	714	875	-0.48%
5,825	854	855	855	855	854	854	854	854	753	859	-0.53%

Table 1: Evolution of OCVs (or average OCVs for packs of 3 or 4 cells) over time for the CSS, as recorded by the eight voltage measurements available of the test bench. OCV_{TH} denotes the theoretical OCV at the time, and Δ_{TOT} the deviation of the OCV at stack level from OCV_{TH}. T_{AO} is the outlet air temperature.

4. Discussion

In review of the results presented in this report, the following sections strive to provide some elements of comparison between the two stack technologies.

- *Performance:*

As expected, the cathode-supported stack (CSS) could reach higher current densities at lower temperatures compared to the electrolyte-supported stack (ESS). For example, the initial performance map indicates that 840°C was necessary for the ESS to reach -0.59 A.cm⁻² in THN70 conditions while the corresponding temperature for the CSS was lower than 670°C, a difference closing in on 200°C. Additionally, the ESS could not be steadily operated at -0.65 A.cm⁻² due to the resulting temperatures too close to the acceptable upper limit, while a thermoneutral current density of -1.55 A.cm⁻² was initially recorded on the CSS at 763°C.

Results also show that the extent of the decrease of thermoneutral current densities over time, akin to apparent degradation, decreases with higher temperature. On the CSS, in about 6,800 h, the performances went down by -63% at about 702°C, while going down by a lesser extent, -58%, at 765°C. This effect is also apparent with the ESS, with a performance drop going from -32% at 780°C to -24% at 840°C in about 7,900 h. When attempting to normalize in respect to duration at comparable temperatures, the degradation rate for CSS at 765°C is estimated around 8.5%.kh⁻¹, while that of the ESS at 780°C is about 4.1%.kh⁻¹. At 840°C, a more relevant temperature for the ESS, the degradation rate is 3.0%.kh⁻¹.

These results emphasize the importance of temperature when evaluating degradation. Consequently, when the cell/stack temperature evolves over time, degradation should be evaluated in regards to a reference temperature [20]. Another way to interpret this result would be to say that 'the rate of temperature increase over time' (when maintaining thermoneutral operation) decreases with higher temperatures. This can be explained by the non-linear temperature dependence of the ASR, which is usually an Arrhenius function, and this nonlinearity increases due to degradation. Hence, at lower temperature the impact of apparent degradation is larger than at higher temperatures.

- *Durability:*

The results show that after 7,900 h, the ESS was closing in on the maximum acceptable temperature. Consequently, had the test continued, the current density would have had to be decreased over time. Contrastingly, after about 6,800 h, only about 760°C were necessary to maintain operation of the CSS at -0.65 A.cm⁻². Extrapolation of the data led to believe in quite a significant remaining lifetime at iso-performance, due to the stack low BoL temperature. However, it is important to underline that extrapolation is not equivalent to practical demonstration. In this view, Sunfire has shown that their stacks could be operated for more than 8,000 h at iso-performance without experiencing sudden, accelerated degradation drivers or catastrophic failures that would have precipitated the stack's EoL. Such statement can only be made up to 6,800 h for the CSS at CEA, the duration of the test presented in this report.

Notably, the temperature-adapting strategy led to iso-performance operation and no production loss was recorded over the complete duration of both experiments (7,900 and 6,800 h respectively).

To emphasize further the statements of iso-performance operation discussed in this work, Figure 5 showcases the evolutions of energy costs of H₂ production at stack level (DC power-to-H₂). Results, only dependent on the operating voltage and not the current density, are indeed stable over time. They are mostly comprised between 34.5 and 35.5 kWh.kgH₂⁻¹. Such range of cost is to be expected with any solid oxide stack technology being operated at the thermoneutral voltage, and is therefore unexpectedly consistent with previously reported data [15]. These results can be compared to 46-48 and 51-54 kWh.kgH₂⁻¹ for PEM and alkaline electrolyses, respectively (assuming operating voltages of 1.7-1.8 V and 1.9-2 V, respectively [21]).

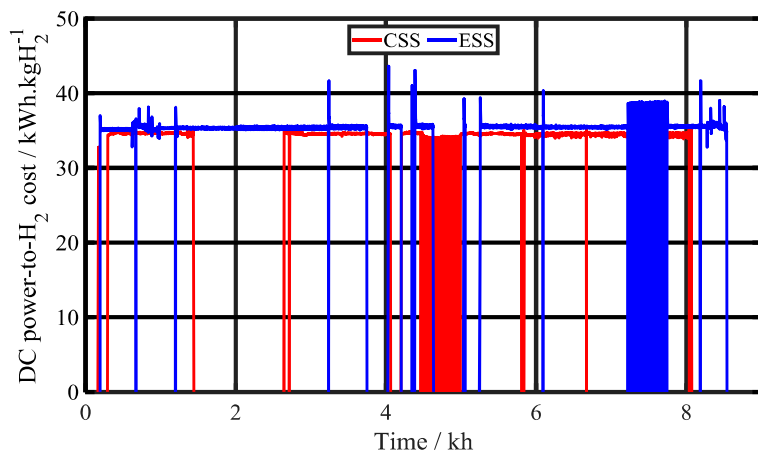


Figure 5: Evolutions of DC power-to-H₂ energy cost for both technologies.

- *Robustness:*

Both stacks showed excellent resilience and came out relatively unscathed of the different malfunction and failure modes that occurred during their respective tests. Notably, no impact of a +300 mbar water head event at the bench inlet on the CSS could be noted. Similarly, while some cells of the ESS were exposed to extreme voltages as a result of multiple failures of the steam generation, only a slight loss of tightness was then evidenced.

Furthermore, the ESS showed an excellent ability to withstand one redox cycle. This result is particularly relevant because if no palliative solution involving forming gas has been implemented at system level, an emergency shutdown could lead to stacks undergoing a redox cycle. An equivalent test was not carried out on the CSS at the end of its test sequence to avoid potential damage that would hinder post-mortem analyses.

- *Overall stack design:*

The design of Sunfire ESS is well suited for industrialization as it allows pile-ups of 4 to 6 units (which has been done already). Indeed, Sunfire has been able to develop compact modules incorporating 24 to 36 stacks to reach high power density.

The design of the CSS used in this test was not intended to be integrated in high power modules. However, significant efforts are on-going to upscale the base design [22].

Conclusions

In order to benchmark different stack technologies, a cathode-supported stack (CSS) and an electrolyte-supported stack (ESS), a harmonized protocol was formulated and implemented in this work. On the one hand, Sunfire has tested 2-30 cell ESS piled-up for 8,200 h. On the other hand, CEA has tested a 25-cell CSS for 6,800 h. The present article aimed at presenting experimental results gathered from over more than 13,000 combined hours, as well as providing some elements of comparison between the two stack technologies.

Performance wise, as expected, the CSS could reach much higher current densities at lower temperature. To reach similar performances on both stacks, the temperature difference was closing in on 200°C at the start of the tests, and 100°C at the end. Significant decrease in performances was recorded on both stack technologies. The extent of the performance drop measured decreased with higher temperatures, emphasizing the importance of that parameter when assessing degradation.

The ESS was operated for more than 8,200 h at iso-performance and -0.5 A.cm^{-2} . Over that time, the temperature was increased to compensate degradation and maintain the stack near an isothermal state, to end up close to the maximum allowed temperature. After about 6,800 h, the CSS temperature associated to -0.65 A.cm^{-2} was 760°C. Over their complete test sequences, both stacks maintained production targets through periodic temperature increase: no hydrogen production loss was recorded.

The results of this article highlight the technical difficulties related to long term testing. Emergencies happened, and components failed. In this view, both stacks showed sufficient resilience and remained relatively unscathed through all events. In addition, the ESS was left mostly unaffected by a redox cycle, which could translate in easier system design and integration.

Finally, the overall ESS design allows pile-ups of several units, and Sunfire has been able to incorporate dozens of stacks into modules of high power density. Conversely, efforts are ongoing to upscale CEA current base design.

Acknowledgment

This project has received funding from the Fuel Cells and Hydrogen 2 Joint Undertaking (now Clean Hydrogen Partnership) under grant agreement No 875123. This Joint Undertaking receives support from the European Union's Horizon 2020 research and innovation programme, Hydrogen Europe and Hydrogen Europe research.

References

- [1] "MultiplHY project website." <https://multiplhy-project.eu/>
- [2] J. Mougín *et al.*, "Development of a Solid Oxide Electrolysis Stack Able to Operate at High Steam Conversion Rate and Integration into a SOE System," *ECS Trans.*, vol. 78, no. 1, pp. 3065–3075, May 2017, doi: 10.1149/07801.3065ecst.
- [3] M. Reytiér, C. Bernard, and P. Giroud, "Stand-alone system for clamping a high-temperature soec/sofc stack," WO2017102657A1, Jun. 22, 2017
- [4] J. Mougín *et al.*, "Enhanced Performance and Durability of a High Temperature Steam Electrolysis Stack," *Fuel Cells*, vol. 13, no. 4, pp. 623–630, Aug. 2013, doi: 10.1002/fuce.201200199.
- [5] M. Reytiér *et al.*, "Development of a Cost-Efficient and Performing High Temperature Steam Electrolysis Stack," *ECS Trans.*, vol. 57, no. 1, pp. 3151–3160, Oct. 2013, doi: 10.1149/05701.3151ecst.
- [6] S. Di Iorio *et al.*, "SOE stack activities at CEA," in *11th European SOFC & SOE Forum*, Lucerne, Switzerland, 2014, vol. B1307, pp. 1–8.
- [7] M. Reytiér *et al.*, "Stack performances in high temperature steam electrolysis and co-electrolysis," *Int. J. Hydrog. Energy*, vol. 40, no. 35, pp. 11370–11377, Sep. 2015, doi: 10.1016/j.ijhydene.2015.04.085.
- [8] J. Aicart, S. Di Iorio, M. Petitjean, P. Giroud, G. Palcoux, and J. Mougín, "Transition Cycles during Operation of a Reversible Solid Oxide Electrolyzer/Fuel Cell (rSOC) System," *Fuel Cells*, vol. 19, no. 4, pp. 381–388, May 2019, doi: 10.1002/fuce.201800183.
- [9] G. Cubizolles, J. Mougín, S. Di Iorio, P. Hanoux, and S. Pylypko, "Stack Optimization and Testing for its Integration in a rSOC-Based Renewable Energy Storage System," *ECS Trans.*, vol. 103, no. 1, pp. 351–361, Jul. 2021, doi: 10.1149/10301.0351ecst.
- [10] A. Hauch, A. Ploner, S. Pylypko, G. Cubizolles, and J. Mougín, "Test and characterization of reversible solid oxide cells and stacks for innovative renewable energy storage," *Fuel Cells*, vol. 21, no. 5, pp. 467–476, Oct. 2021, doi: 10.1002/fuce.202100046.
- [11] A. Chatroux *et al.*, "A Packaged and Efficient SOEC System Demonstrator," *ECS Trans.*, vol. 68, no. 1, pp. 3519–3526, Jul. 2015, doi: 10.1149/06801.3519ecst.
- [12] A. Chatroux *et al.*, "Power to Power efficiencies based on a SOFC/SOEC reversible system," in *12th European SOFC & SOE Forum*, Lucerne, Switzerland, Jul. 2016, vol. B1104, pp. 222–230.
- [13] "SOCTESQA." <http://www.soctesqa.eu/>
- [14] J. Aicart, L. Tallobre, A. Surrey, D. Reynaud, and J. Mougín, "Experimental Report on Galvanostatic Operation of Electrolyte-Supported Stacks for High Temperature Electrolysis," in *15th European SOFC & SOE Forum*, Lucerne, Switzerland, May 2022, vol. A0808, pp. 1–12.
- [15] J. Aicart *et al.*, "Performance evaluation of a 4-stack solid oxide module in electrolysis mode," *Int. J. Hydrog. Energy*, p. S0360319921044360, Nov. 2021, doi: 10.1016/j.ijhydene.2021.11.056.
- [16] M. Lang, S. Raab, M. S. Lemcke, C. Bohn, and M. Pysik, "Long Term Behavior of Solid Oxide Electrolyser (SOEC) Stacks," *ECS Trans.*, vol. 91, no. 1, pp. 2713–2725, Jul. 2019, doi: 10.1149/09101.2713ecst.
- [17] M. Riedel, M. P. Heddrich, and K. A. Friedrich, "Analysis of pressurized operation of 10 layer solid oxide electrolysis stacks," *Int. J. Hydrog. Energy*, vol. 44, no. 10, pp. 4570–4581, Feb. 2019, doi: 10.1016/j.ijhydene.2018.12.168.
- [18] M. Preininger, B. Stoeckl, V. Subotić, F. Mittmann, and C. Hochenauer, "Performance of a ten-layer reversible Solid Oxide Cell stack (rSOC) under transient